

Transcriptomic and metabolic analysis uncovers the role of light quality in carotenoid accumulation of grapefruit during ripening

Liulian Huang

Southwest University

Linping Hu

Southwest University

Wenbin Kong

Chongqing Agricultural Technology Extension Station

Can Yang

Southwest University

Wanpeng Xi (✉ xwp1999@zju.edu.cn)

southwest university

Article

Keywords: grapefruit, light, bagging, carotenoid, RNA-sequencing, WGCNA

Posted Date: August 31st, 2021

DOI: <https://doi.org/10.21203/rs.3.rs-825511/v1>

License:  This work is licensed under a Creative Commons Attribution 4.0 International License.

[Read Full License](#)

Version of Record: A version of this preprint was published at Communications Biology on April 4th, 2022. See the published version at <https://doi.org/10.1038/s42003-022-03270-7>.

1 **Transcriptomic and metabolic analysis uncovers the role of light quality in**
2 **carotenoid accumulation of grapefruit during ripening**

3 Running Head: Light changes carotenoid accumulation in grapefruit

4

5 **Xiulian Huang^{a#}, Linping Hu^{a#}, Wenbin Kong^b, Can Yang^a, Wanpeng Xi^{a*}**

6

7 ^a College of Horticulture and Landscape Architecture, Southwest University,

8 Chongqing 400716, China

9 ^b Chongqing Agricultural Technology Extension Station, Chongqing 401121, China

10 ^c Key Lab of Aromatic Plant Resources Exploitation and Utilization in Sichuan

11 Higher Education, Yibin University, Yibin, Sichuan 644000, China

12

13 *Correspondence author

14 E-mail address: xwp1999@zju.edu.cn

15 Postal address: College of Horticulture and Landscape Architecture, Southwest

16 University, Chongqing China 400716

17

18 [#]These authors contributed equally to this work.

19

20

21

22

23 **Abstract**

24 Light, a crucial environmental signal, is involved in the regulation of secondary
25 metabolites. To understand the mechanism by which light influences carotenoid
26 metabolism, grapefruits were bagged with four types of light-transmitting bags that
27 altered the transmission of solar light. We showed that light-transmitting bagging
28 induced changes in carotenoid metabolism during fruit ripening. Compared with natural
29 light, red light (RL)-transmittance treatments significantly increased the total
30 carotenoid content by 142%. Based on weighted gene co-expression network analysis
31 (WGCNA), ‘red’, ‘darkred’, ‘yellow’, ‘brown’ and ‘midnightblue’ modules were
32 remarkably associated with carotenoid metabolism under different light treatment.
33 Transcriptome analysis identified the transcription factors (TFs) bHLH74/91/122,
34 NAC56/78/90/100, MYB/MYB308, WRKY7/55, MADS29/AGL61, ERF043/118 as
35 being involved in the regulation of carotenoid metabolism in response to RL. Under RL
36 treatment, these TFs regulated the accumulation of carotenoids by directly modulating
37 the expression of carotenogenic genes, including *PSY*, *Z-ISO2*, *ZDS6*, *LCYB*, *LCYE*,
38 *CHYB*, *CCD1-1/1-3*, *CCD4-2* and *NCED2/3*. Based on these results, a network of the
39 regulation of carotenoid metabolism by light in citrus fruits was preliminarily proposed.
40 These results showed that RL treatments have great potential to improve coloration and
41 nutritional quality of citrus fruits.

42

43 **Keywords:** grapefruit, light, bagging, carotenoid, RNA-sequencing, WGCNA.

44

45

46

47

48

49

50 **Introduction**

51 Carotenoids are a large class of natural lipid-soluble pigments that are extensively
52 distributed in plants and play important roles in plant growth and development, being
53 involved in photosynthesis, photomorphogenesis, photoprotection, and phytohormone
54 synthesis^{1,2}. The accumulation of carotenoids confers on many fruits and vegetables
55 their various colors, such as yellow, orange, and red hues³. In addition, their catabolites
56 provide precursors for the synthesis of abscisic acid (ABA) and strigolactones (SLs),
57 which participate in various biological processes and stress responses⁴. In humans,
58 carotenoids in plant-based foods are an important source of dietary vitamin A, which is
59 essential for health and nutrition, and carotenoid-rich diets are correlated with a
60 significant reduction in the risks of chronic diseases such as cancers, cardiovascular
61 diseases, and several degenerative diseases^{2,5}. The concentrations of carotenoids in
62 fleshy fruits thus greatly influence their commercial and nutritional value.

63 The grapefruit (*Citrus paradisi* Macf.) is an economically important tropical
64 cultivated citrus fruit⁶. In 2018, the planted area of grapefruit in China was about 9200
65 hectares, about 25% of the global planted area, while annual production (around 5
66 million tons) accounted for approximately 54% of global output, indicating that
67 grapefruit is an important part of China's citrus production (FAO statistics,
68 <http://www.fao.org/home/en/>). Red grapefruit is becoming more and more preferred by
69 consumers for its unique flavor and attractive pulp color. Besides having an abundance
70 of a wide variety of health-promoting compounds such as flavonoids, dietary fiber, and
71 vitamin C⁷, grapefruits are richer in carotenoids than other citrus species and thus

72 represent an ideal material for investigating carotenoid metabolism.

73 The pathway of carotenoid biosynthesis has been clearly established in plants⁸.
74 The five-carbon prenyl diphosphate isopentenyl diphosphate (*IPP*) and its double-bond
75 isomer dimethylallyl diphosphate (*DMAPP*) are synthesized in plastids via the 2-C-
76 methyl-D-erythritol 4-phosphate (MEP) pathway. The subsequent condensation of two
77 molecules of geranylgeranyl diphosphate (*GGPP*), produced from *IPP* and *DMAPP*,
78 by phytoene synthase (*PSY*) generates the colorless 15-*cis*-phytoene. After sequential
79 desaturation and isomerization reactions catalyzed by phytoene desaturase (*PDS*) and
80 ζ -carotene desaturase (*ZDS*), and ζ -carotene isomerase (*Z-ISO*) and ζ -carotenoid
81 isomerase (*CRTISO*), respectively, phytoene is converted into the red all-trans-
82 lycopene⁹. The production of α - and β -carotene from lycopene involves a set of
83 cyclization reactions catalyzed by lycopene ϵ -cyclase (*LCYE*) and lycopene β -cyclase
84 (*LCYB*) or *LCYB* alone, representing the β , ϵ - and β , β -branches of the pathway,
85 respectively, and this step is the pivotal branch point in carotenoid metabolism. Next,
86 α -carotene is converted into lutein by β -ring hydroxylase (*CYP97A*) and ϵ -ring
87 hydroxylase (*CYP97C*) of the cytochrome P450 family. The production of zeaxanthin
88 from β -carotene is catalyzed by β -carotene hydroxylase (*CHYB*), and violaxanthin is
89 generated via antheraxanthin by zeaxanthin epoxidase (*ZEP*). The cleavage of
90 carotenoids is catalyzed by the proteins of carotenoid-cleavage genes (*CCD* or *NCED*),
91 producing apocarotenoids such as β -ionone, β -citraurin, and ABA^{1,3}.

92 Carotenoid biosynthesis and degradation are coordinated by a range of enzymes
93 encoded by structure genes and transcription factors (TFs)⁸. These structure genes have

94 been identified and isolated in many plant species to date^{3,8}. However, only a few
95 transcription factors related to carotenoid metabolism have been identified in plants,
96 including RIPENING INHIBITOR (RIN) and FRUITFULL1/2 (FUL1/2) in the
97 MADS-box family; PIF1, TOMATO AGAMOUS LIKE1 (TAGL1), SIMADS1,
98 SINAC1/4, SIAP2a, SIERF6, and SIBBX20 in tomatoes¹⁰⁻¹²; CsMADS5/6 and
99 CrMYB68 in oranges (flavedo)¹³⁻¹⁵; CpEIN3a, CpNAC1/2, and CpbHLH1/2 in
100 papaya¹⁶⁻¹⁸; AdMYB7 in kiwifruits¹⁹; and R2R3-MYB subgroup Reduced Carotenoid
101 Pigmentation 1/2 (RCP1/2) in monkey flower species^{12,20}. Compared with that of
102 anthocyanin metabolism, the transcriptional regulation of carotenoid metabolism is far
103 from understood.

104 Light not only provides the energy required for photosynthesis but also participates
105 in the regulation of a variety of metabolic processes as the crucial medium for the
106 exchange of information between the plant and external environment during
107 development^{21,22}. An increasing number of investigations suggest that light signals also
108 play a fundamental role in secondary metabolism in fruit. However, the majority of
109 studies have focused on the effect of postharvest light treatment on fruit quality, with
110 only a few referring to the impact of developmental light treatment on fruit quality²³.
111 As an effective method of protecting fruit from insect infestations, bird attack, and
112 sunburn as well as reducing disease incidence rate and chemical residues, fruit bagging
113 is extensively used in modern orchards²⁴. Light-transmitting paper bags of different
114 colors can absorb the light waves of the corresponding colors, making their use a
115 feasible approach for investigation of how light influences phytochemicals metabolism

116 during fruit development.

117 This study was carried out to know the role of light quality on the carotenoid
118 accumulation in grapefruit and understand the transcriptional regulatory mechanism
119 underlying light signals during fruit ripening. The carotenoid level of ‘Huoyan’
120 grapefruit pulp treated with different light-transmittance during the ripening were
121 compared, WGCNA were employed to identify the key genes and TFs responsible for
122 carotenoid metabolism during the process. Based these results, a regulatory network of
123 carotenoid metabolism in response to red-light was preliminarily proposed. These
124 findings provide new insight into carotenoid metabolism and demonstrate a potential
125 approach for improvement of the coloration and nutritional quality of citrus fruit and
126 other horticultural crops.

127

128 **Results**

129 **Effects of light transmittance on TSS, TA, and CCI during fruit ripening**

130 Compared with that in the dark shade treatment (DS), the TSS content of the grapefruits
131 treated with RL, BL, and WL gradually increased during fruit ripening and were
132 significantly higher than that in DS treatment at 215 DAB ($p < 0.05$) (**Fig. 1A**). The
133 effect of light treatment on TA content is different (**Fig. 1B**). It is worth noting that the
134 TA content under RL and WL treatment slightly rose during fruit ripening while the TA
135 content gradually decreased in BL and DS treatment. CCI shared similar trends and
136 were gradually increased in all light treatments (**Fig. 1C**).

137

138 **Effects of light transmittance on carotenoid accumulation during fruit ripening**

139 Five major carotenoids were identified from ‘Huoyan’ grapefruit pulp, including β -
140 carotene, phytofluene, ζ -carotene, lycopene, and 9-*cis*-violaxanthin (**Table S1**). The
141 carotenoid profiles differed in the four light treatments, and the ‘Huoyan’ grapefruit
142 pulp was rich in β -carotene and lycopene (**Fig. 2**). Compared with the control group
143 (DS), the total carotenoid content was the highest in the grapefruits treated with RL
144 (2.4-fold), followed by the grapefruits treated with BL (1.69-fold) and WL (1.59-fold)
145 at 215 DAB. Subsequently, we found that the content of β -carotene, ζ -carotene lycopene
146 and phytofluene gradually increased as fruit ripening under different light treatments
147 while 9-*cis*-violaxanthin content didn’t show marked changes. Compared with DS, the
148 β -carotene and lycopene content significantly increased under RL treatment and
149 remarkably higher than those in BL and WL treatment at 215 DAB.

150

151 **Transcriptome profiles during fruit ripening**

152 Average clean reads number of mRNA libraries for eight samples ranged from 20.98 to
153 23.09 million (**Table S2**). The alignment of the clean reads against the reference
154 genome and reference gene sequences generated a total of 25,694 unigenes (**Table S3**).
155 In four light treatments, the median of gene expression level ranged from 0.76 to 0.88
156 and there were differences between the samples (**Fig. S2**). The fruit samples in BL
157 treatment showed the lowest median, 0.76, at 215 DAB, while the samples treated with
158 WL presented the biggest median value of 0.88 at 185 DAB. However, in the DS and
159 RL treatment groups, the gene expression levels for samples were relatively stable

160 during ripening.

161

162 **Identification of differentially expressed genes (DEGs)**

163 Based on RNA sequencing results, a total of 5541 DEGs were identified during fruit
164 ripening, with 2305, 1381 and 1855 DEGs showing differential expression between DS
165 and RL, DS and BL, and DS and WL, respectively (**Fig. 3A**). In the RL group, 1817
166 and 488 DEGs were identified at 185 and 215 DAB, respectively, and the number of
167 DEGs was significantly higher than other light treatments. The numbers of extremely
168 significant DEGs throughout fruit ripening were 152, 167 and 173, respectively, after
169 RL, BL, and WL treatment (**Fig. 3B**). Notably, at the two indicated detection points, the
170 unique DEGs of RL, BL and WL treatment, respectively, reached a maximum of 1650
171 at 185 DAB, 598 DEGs at 215 DAB and 1159 DEGs at 185 DAB.

172

173 **Weighted gene co-expression network analysis (WGCNA)**

174 The WGCNA was performed using 12619 unigenes (FPKM > 1, the top 50% of
175 variance), which were classified into twenty-four modules (**Fig. 4**), of which the ‘red’,
176 ‘darkred’, ‘yellow’, ‘brown’ and ‘midnightblue modules were remarkably associated
177 with carotenoid metabolism under different light condition during fruit ripening ($p <$
178 0.05). The analysis of the correlation between gene expression and carotenoid
179 accumulation demonstrated that the ‘red’ and ‘darkred’ module, respectively, contained
180 469 (3.7%) and 53 (0.4%) genes and was significantly positively correlated with the
181 content of carotenoid. Besides, ‘yellow’ module was positively associated with

182 phytofluene content ($r=0.78$, $p=0.02$). However, ‘brown’ and ‘midnightblue’ modules
183 were highly negatively related with phytofluene content, which contained 1882 genes
184 (14.9%), with a correlation coefficient of -0.75 ($p = 0.03$) and -0.72 ($p = 0.04$),
185 respectively. These results indicate that genes in these modules were potentially
186 correlated with carotenoid accumulation under different light conditions.

187

188 **Expression analysis of genes related to carotenoid metabolism**

189 In the carotenoid metabolic pathway (**Fig. 5a**), a total of eight structural genes,
190 including *GGPPS1*, *ZEP1/2*, *CCD1-1/1-3*, *CCD4-1*, *NCED2/3*, were differentially
191 expressed in response to RL during ripening (**Table S4**). RL significantly induced the
192 transcription for carotenoid biosynthetic and cleavage genes during grapefruit ripening
193 (**Fig. 5A**). Among the 3080 genes in the carotenoid co-expression modules, a total of
194 235 transcription factors (TFs), which were enriched in 52 gene families such as ERF
195 (21), bHLH (19), MYB (18), WRKY (15), NAC (9) and MADS (7), were identified
196 (**Fig. S3**). In order to further excavate the transcription factors responding to RL, we
197 screened the differentially expressed transcription factors between RL and DS group.
198 In order to further excavate the transcription factors responding to RL, we screened the
199 differentially expressed transcription factors between RL and DS group. Subsequently,
200 a total of forty-eight differentially expressed TFs in response to RL, including ERF (13),
201 WRKY (7), bHLH (5), NAC (4), C3H (4), bZIP (4), MYB (3), GRAS (3), HSF (2), Dof
202 (2), MADS (2) and GRF (1), were identified as candidate TFs modulating carotenoid
203 biosynthesis in response to RL during fruit ripening (**Fig. 5B, Table S5**).

204

205 **Visualization of gene networks**

206 In order to identify the hub gene underlying carotenoid metabolism under different
207 light-transmittance conditions, the co-expression for structural genes and regulators
208 was visualized using Cytoscape. In carotenoid co-expression modules, forty TF
209 members—derived from the ERF (10), WRKY (9), bHLH (5), bZIP (4), NAC (3), MYB
210 (3), C3H (2) Dof (2), GRAS (1) and GRF (1) families—were identified as the key genes
211 related to carotenoid metabolism. Meanwhile, twelve structural genes, namely *IPI*, *PDS*,
212 *ZDS4/ZDS7*, *CRTISO1/3*, *CYP97C1/2*, *CCD1-2*, *CCD4-2*, *CCS*, *NXS*, which directly
213 involved in the carotenoid biosynthesis and cleavage, were identified as the key
214 regulatory genes in co-expression network (**Fig. 6**). In addition, we found that thirty-
215 two TFs, including ERF, WRKY, bHLH, NAC and MYB family members were co-
216 expressed with carotenoid cleavage gene *CCD4-2* and six TFs had a co-expression
217 relationship with *CYP97C1* (**Table S6**). Notably, there was a co-expression relationship
218 between MYB4 and *CCD1-2*, *CCS*, *PDS*. These results suggested that above
219 transcription factors and structural genes might interact with each other to regulate the
220 flux for carotenoid in grapefruits.

221

222 **Discussion**

223 Light signals play a vital role in carotenoid metabolism.^{22,25} Although many studies
224 have investigated the effects of postharvest light treatments, such as LED, pulse, and
225 ultraviolet light, on carotenoid metabolism²⁶⁻²⁸, the role of light quality in carotenoid

226 metabolism underlying fruit ripening previously had not been elucidated. In this work,
227 different light-transmittance bagging treatments were used to understand the influence
228 of light quality on grapefruits throughout the ripening process at the metabolic and
229 molecular levels.

230 Existing research indicates light irradiation modulates the biosynthesis and
231 catabolism of carotenoids in fruit and modifies the concentration and composition of
232 carotenoids^{25,29}. The total carotenoid content was reduced upon ripening in covered
233 tomatoes and peppers²³. In grapefruit peel, an unusual pattern of lycopene accumulation
234 in might be associated with the developmentally regulated differentiation of
235 chromoplasts mediated by light²⁹. Light deprivation promoted peel degreening and
236 reduced carotenoid accumulation in mandarins and sweet orange fruits²⁵. In contrast,
237 light irradiation enhanced carotenoid accumulation and external quality during
238 mandarin fruit development³⁰. Here, our results showed that carotenoid (total
239 carotenoid, β -carotene, phytofluene, and lycopene) accumulation was significantly
240 induced by red-transmittance bagging treatments (**Fig. 2**), suggesting that RL played
241 significant positive role in carotenoid accumulation in grapefruit pulp. These are
242 evidence of the promotion of carotenoid metabolism by light in fruit.

243 Lighting factors can regulate secondary metabolism by light quality, light intensity,
244 and light irradiation time in plant²³. Red LED light (660 nm) activated the expression
245 of *VvNCED1* in ripening grape skin (*Vitis vinifera* L.)³¹, but had no effect on the
246 carotenoid content of citrus juice sacs. Blue LED light (470 nm) treatment stimulated
247 carotenoid accumulation by upregulating the expression of the *CitPSY* gene in the juice

248 sacs of three citrus varieties (mandarin (*Citrus unshiu* Marc.), Valencia orange (*C.*
249 *sinensis* Osbeck) and Lisbon lemon (*C. limon* Burm.f.)³². In the present study, we found
250 that RL promoted lycopene and β -carotene accumulation along with upregulation of
251 *PSY*, *Z-ISO1/2*, *ZDS1/6*, *LCYB*, *LCYE*, *NCED3* and *CCD1-3* (**Fig. 2 and 5**), which was
252 similar with the upregulation of the *PSY* gene induced by continuous red light in
253 *Arabidopsis thaliana* seedlings, leading to increases in carotenoid content³³. However,
254 blue- and white-light transmittance treatment have no significant effect on carotenoid
255 content during grapefruit ripening. These results revealed that the regulatory roles of
256 light in carotenoid metabolism also depends on the light quality.

257 A large number of TFs have been reported to be involved in carotenoid metabolism
258 via transcriptional regulation of key structural genes in plant. Here, multiple members
259 of ERF, NAC, WRKY, MYB, MADS, bHLH families be identified as hub genes for
260 modulating carotenoid flux (**Fig. 5 and 6**). Work in *Arabidopsis thaliana* revealed that
261 the PIF1 (phytochrome interacting factor 1) transcription factor suppressed *PSY*
262 transcript by directly binding the G-box motifs and further regulated carotenoid
263 metabolism³⁴. Zhou et al. showed that CpbHLH1/2 promoted lycopene degradation to
264 carotenoids by upregulating the transcripts of the lycopene β -cyclase genes (*CpLCYB*
265 and *CpCHYB*) in response to strong light during papaya ripening¹⁸. Blue- and red-light
266 supplementation irradiation to tomato fruits at anthesis facilitated lycopene biosynthesis,
267 which was considered to be related with regulation of the photoreceptor HY5
268 (ELONGATED HYPOCOTYL5) and PIFs upon the expression of *PSY1*³⁵. Here, in RL-
269 treated grapefruit, bHLH62/74/91/122 in 'brown' module negatively correlated with

270 phytofluene presented markedly down-regulated trend coupled with transcript increase
271 of *PSY* and *CHYB* (**Fig. 2, 5 and 7**), which accounted for higher phytofluene level, and
272 these results are paralleled with carotenoid increase of content in SIPIF4-silenced
273 tomato³⁶.

274 Some ripening related regulators have been shown the regulatory role in
275 carotenoid metabolism. In tomato, MADS-box TFs *RIN* gene was reported to
276 specifically regulating accumulation of lycopene by positively regulated carotenoid
277 biosynthetic genes (including *PSY*, *Z-ISO*, *CRTISO*) and negatively regulated
278 carotenoid downstream genes *LCYB* and *LCYE*, while *FUL* homologs *FUL1/2*
279 regulated overall carotenoid pathway by targeted multiple carotenogenic genes^{37,38}. In
280 sweet orange (*Citrus sinensis*), *CsMADS5/6* activated expression for carotenogenic
281 genes, including *PSY*, *PDS*, *LCYb1/CCD1* via directly binding its promoter and thus
282 modulated carotenoid metabolism^{13,14}. In ‘darkred’ module, we found that up-
283 regulation of *MADS29* in response to RL was accompanied by the increased expression
284 level of *Z-ISO2*, *LCYB* as well as *CCD1-3*, which facilitated carotenoid accumulation
285 (**Fig. 2, 5 and 7**). By contrast, the significantly reduced expression of *AGL61* for
286 ‘darkred’ module during ripening suggested their negative correlation with phytofluene
287 accumulation in grapefruit (**Fig. 5 and 7**). Recently, *PpERF3* has been shown to be
288 involved in ABA biosynthesis by activating *PpNCED2/3* transcription during peach
289 fruit ripening³⁹. Here, *PpERF3* homolog *ERF012* was down-regulated in response to
290 RL, which suggested *ERF012* were highly likely to be involved in carotenoid process
291 mediated by RL. On the contrary, RL remarkably promoted transcript of *ERF043/118*

292 and *NCED2/3* shared similar expression patterns with them (**Fig.5 and 7**). Above
293 analysis indicated ERF TFs differently respond to RL and collaboratively regulated
294 carotenoid accumulation. In the *Arabidopsis*, suppression of AtRAP2.2 leads to
295 reduction of *PSY* and *PDS* transcript⁴⁰. In rice leaves, AP2/ERF genes were negatively
296 associated with carotenoid accumulation under both blue- and red-light treatments⁴¹.
297 Here, we also found multiple ERF TFs (ERF023-like/025/026) in ‘brown’ module
298 displayed negative correlation with phytofluence accumulation in response to RL.

299 Another fruit ripening related TF NACs were also reported to be involved in
300 carotenoid metabolism. In tomato SINAC4/19/48 RNAi fruit, the transcript levels of
301 *PSY* were reduced and thus resulted in decreased lycopene^{42,43}. However, the
302 overexpression of SINAC1 reduced lycopene content, which was associated with a
303 reduction in *SIPSY* and an increase in *SILCYB* and *SILCYE* expression⁴⁴. During papaya
304 fruit ripening, CpNAC2 co-operated with CpEIN3a to promote *CpPDS2/4*, *CpZDS*,
305 *CpCHYB*, and *CpLCYE* transcription, accounting for the elevated carotenoid contents¹⁷.
306 CcNAC1/2 were transcriptionally upregulated under red-light treatment in *Citrullus*
307 *colocynthis*⁴⁵. Similarly, FcrNAC22 upregulated carotenoid metabolism and ABA
308 synthesis via activation of *FcrLCYB1*, *FcrBCH2* and *FcrNCED5* in RL-irradiated
309 fruits⁴⁶. Here, we observed that the increased expression levels of NAC56 (the
310 SINAC48 homolog) and NAC100 mediated by RL were positively related with
311 expression of up-stream genes (*PSY*, *Z-ISO2*, *ZDS6*, *LCYB* and *LCYE*) in carotenoid
312 metabolic pathway, while downregulated NAC68/78/90 showed a negative correlation

313 with transcript for these genes, consistent with lycopene accumulation in ripening
314 grapefruit fruit (**Fig. 2, 5 and 7; Fig. S4**).

315 Some publications in recent years have reported that MYB TFs played a positive
316 role in carotenoid regulation. In the flavedo of *Citrus reticulata*, CrMYB68 indirectly
317 inhibited the transformation of α/β -carotene via negative regulation for *CrBCH2* and
318 *CrNCED5*¹⁵. AdMYB7 was positively correlated with *AdLCYB* in terms of expression
319 and further regulated carotenoid biosynthesis¹⁹. In ‘darkred’ module, we found that
320 MYB308 induced by RL was also positively correlation with carotenoid accumulation,
321 especially lycopene, during grapefruit ripening (**Fig. 4 and 5**). Additionally, seven
322 WRKY TFs were differentially expressed in response to RL during grapefruit ripening
323 (**Fig. 5**). In *Osmanthus fragrans*, OfWRKY3 was found to be a positive regulator of the
324 *OfCCD4* gene via binding to its W-box palindrome motif⁴⁷. In this study, we also
325 observed that two WRKY TFs, namely WRKY7/55 were gradually down-regulated as
326 grapefruit fruit ripening, accompanied by the reduction of *CCD4-2* expression of in RL
327 treatment (**Fig. 2, 5 and 7**). Besides, RL also notably suppressed expression for C3H
328 (2), bZIP (4) and Dof (2) TFs in ‘brown’ module, suggested these TFs might involve in
329 carotenoid accumulation (**Fig. 5**).

330

331 **Conclusion**

332 In present study, the carotenoid accumulation in grapefruit respond differently to light
333 quality, RL have the significant inducing role during fruit ripening. The process was
334 modulated by multiple TFs (bHLH74/91/122, NAC56/78/90/100, MYB/MYB308,

335 WRKY7/55, MADS29/AGL61, ERF043/118,) as well as carotenogenic genes (*PSY*, *Z-*
336 *ISO2*, *ZDS6*, *LCYB*, *LCYE*, *CHYB*, *CCD1-1/1-3*, *CCD4-2* and *NCED2/3*), and a
337 preliminary regulatory model of red light-induced carotenoid metabolism in grapefruits
338 was established (**Fig. 7**). These findings not only provide new insight into the regulation
339 of carotenoid metabolism, but also offer an effective approach for enhancing the quality
340 of citrus fruits in agricultural practice.

341

342 **Materials and methods**

343 **Plant materials and treatments**

344 ‘Huoyan’ grapefruit were cultivated at the National Citrus Germplasm Repository of
345 the Citrus Research Institute at the Chinese Academy of Agricultural Sciences in
346 Chongqing, China and used as experimental materials. Trees with the same age, tree
347 structure, and identical growth conditions were selected for the experiment and
348 cultivated under the same management condition. Grapefruits with similar sizes and
349 colors from outside of tree were bagged with four different light-transmitting paper bags
350 at 120 days after blossom (DAB)—red-light-transmitting bags (RL) (peak wavelength,
351 748 nm), blue-light-transmitting bags (BL) (peak wavelength, 478 nm), and white-
352 light-transmitting bags (WL), and a dark-shading bag (DS) was as the control (**Fig. S1**).
353 Fruits of a uniform size were picked at 185 (maturation) and 215 (fully ripe) days after
354 blossom (DAB). Each fifteen fruits were as one replicate and three biological replicates
355 were used for each sample point of every treatment. After determining the basic
356 physiological parameters, the fruits were cut into small cubes, frozen using liquid

357 nitrogen, and stored at $-80\text{ }^{\circ}\text{C}$ for further analysis.

358

359 **Determination of basic physiological parameters**

360 The fruit color parameters were measured using the Hunter Associates Laboratory
361 Scanner (Hunter Associates Laboratory, Inc., Reston, VA, USA). The citrus color index
362 (CCI) for the mesocarp was calculated according to the formula $\text{CCI} = 1000 \times a^* / (L^* \times b^*)$, using five fruits as a single replicate and three biological replicates were used for
363 each sample. To determine the total soluble solid (TSS) content, 200 μL of fresh
364 squeezed juice was obtained from juice sacs and then analyzed with a digital hand-held
365 refractometer (Atago PR-101R, Atago, Japan). Titratable acidity (TA) was measured
366 after the juice sample was diluted 50 times with purified water.

368

369 **Extraction and identification of carotenoids**

370 Carotenoids were identified following our previously described method⁴⁸. Ten grams
371 of pulp powder was extracted with 20 mL of solvent (hexane/acetone/ethanol, 50:25:25,
372 v/v/v) in a screw-top tube. The colored top layer was recovered and dried with nitrogen
373 gas after being left to stand for 30 min, protected from light. After saponification, 2 mL
374 of 1% butylhydroxytoluene (BHT)/methyl tert-butyl ether (MTBE) was added to the
375 colored layer, and the mixture was filtered through sodium sulfate into a brown bottle
376 for drying. The residue was dissolved in 2 mL of methanol/acetone (2:1, v/v) for HPLC
377 analysis.

378 The carotenoids were identified by HPLC (Waters, Milford, MA, USA) with a C_{30}

379 chromatography column (250 × 4.6 mm, 5 μm; YMC, Wilmington, NC, USA). The
380 mobile phases for the carotenoids were composed of MTBE (A), methanol (B), and an
381 aqueous phase (C) and were prepared by a multistep linear gradient elution. The
382 identification was performed by comparing the retention times and UV–visible spectral
383 peaks between the samples and standards. The carotenoid contents were calculated
384 according to a standard curve based on authentic compounds and are expressed herein
385 as mg/kg fresh weight (FW).

386

387 **Library construction, transcriptome sequencing, and gene annotation**

388 Total RNA was extracted using an Agilent RNA 6000 Nano kit (Agilent, CA, USA)
389 according to the manufacturer’s instructions, the RNA concentration and integrity were
390 assessed using an Agilent 2100 Bioanalyzer, and the OD260/OD280 and
391 OD260/OD230 values were determined using a NanoDrop 2000 spectrophotometer
392 (NanoDrop 2000, Wilmington, DC, USA) to assess the RNA purity. Eight mRNA
393 libraries were constructed for RNA-seq of the pulp samples harvested at 185 and 215
394 DAB. Three biological replicates were performed for each sample.

395 The libraries were sequenced on an Illumina HiSeq™ 2000 system at the Beijing
396 Genomics Institute (BGI), China. The raw sequencing data were filtered by removing
397 adaptors, low-quality and redundant sequences, and reads with unknown “N” base
398 content higher than 5% using the SOAPnuke (version 1.4.0) and Trimmomatic (version
399 0.36) software. The clean reads were aligned to the reference genome database using
400 HISAT (version 2.1.0)⁴⁹.

401 For transcription factor annotation, open reading frames (ORF) were obtain
402 ed from the quality-checked data using getorf (EMBOSS: 6.5.7.0, [http://emboss.](http://emboss.sourceforge.net/apps/cvs/emboss/apps/getorf.html)
403 [sourceforge.net/apps/cvs/emboss/apps/getorf.html](http://emboss.sourceforge.net/apps/cvs/emboss/apps/getorf.html), -minsize 150) and aligned to Pl
404 ant Transcription Factor Database (<http://plantfdb.gao-lab.org/blast.php>).

405

406 **Identification of differentially expressed genes (DEGs)**

407 The RSEM software package (version 1.2.8,
408 <http://deweylab.biostat.wisc.edu/rsem/rsem-calculate-expression.html>) was used to
409 calculate expression levels for transcripts with the default parameters⁵⁰. The
410 expression levels are expressed as FPKM values. The genes that were differentially
411 expressed between two samples were determined as previously described according to
412 the Poisson distribution and the algorithm developed by BGI⁵¹. The DEGs ($p \leq 0.005$;
413 $|\log_2 \text{fold change}| \geq 1$; $\text{FDR} \leq 0.001$) were then screened for further analysis.

414

415 **Weighted gene co-expression network analysis (WGCNA) and network** 416 **visualization for candidate genes**

417 A total of 16831 unigenes with FPKM values > 1 were utilized to conduct weighted
418 gene co-expression network analysis using WGCNA⁵², reshape2 and stringr packages
419 in Rstudio (v1.4.1717, <https://www.rstudio.com/products/rstudio/download/>). To
420 reduce the size of the data calculation, a total of 12619 unigenes with the first 75%
421 variance were screened from the above unigenes with unsigned TOM type to build a
422 co-expression network. The phenotypic data regarding the carotenoids in the pulp were

423 associated with the constructed co-expression network to screen the modules that were
424 significantly correlated with carotenoid metabolism ($p \leq 0.05$). Finally, DEGs were
425 imported into the cytoscape software (version 3.7.2,
426 <https://cytoscape.org/download.html>) for network visualization.

427

428 **Acknowledgements**

429 This work was supported by the National Science Foundation of Chongqing for
430 Distinguished Young Scholars (No. cstc2019jcyjqq0029).

431

432 **Data availability**

433 The transcriptome raw reads have been deposited as a BioProject
434 (<https://submit.ncbi.nlm.nih.gov/subs/sra/>) under accession number: PRJNA728380.

435

436 **Author contributions**

437 W.X. designed the project. X.H. prepared the manuscript. L.H. analyzed the data. W.K.
438 and W.Z participated in collecting the materials. C.Y., L.H., and X.H. participated in
439 assaying the physiological parameters.

440

441 **Competing interests**

442 The authors declare no competing interests

443

444 **Additional information**

445 Supplementary information

446

447 **References**

- 448 1. Sun, T. et al. Carotenoid metabolism in plants: the role of plastids. *Mol. Plant* **11**,
449 58-74 (2018).
- 450 2. Rowles, J. L. & Erdman, J. W. Carotenoids and their role in cancer prevention.
451 *Biochim. Biophys. Acta Mol. Cell Biol. Lipids* **1865**, 158613 (2020).
- 452 3. Nisar, N., Li, L., Lu, S., Khin, N. C. & Pogson, B. J. Carotenoid metabolism in
453 plants. *Mol. Plant* **8**, 68-82 (2015).
- 454 4. Jia, K. P., Baz, L. & Al-Babili, S. From carotenoids to strigolactones, *J. Exp. Bot.*
455 **69**, 2189-2204 (2018).
- 456 5. Fanciullino, A. L., Bidel, L. P. R. & Urban, L. Carotenoid responses to
457 environmental stimuli: integrating redox and carbon controls into a fruit model.
458 *Plant Cell Environ.* **37**, 273-289 (2014).
- 459 6. Corazza-Nunes, M. J., Machado, M. A. & Nunes, W. M. C. Cristofani M and
460 Targon MLPN, Assessment of genetic variability in grapefruits (*Citrus paradisi*
461 Macf.) and pummelos (*C. maxima* (Burm.) Merr.) using RAPD and SSR markers.
462 *Euphytica* **126**, 169-176 (2002).
- 463 7. Zou, Z., Xi, W., Hu, Y., Nie, C. & Zhou, Z. Antioxidant activity of citrus fruits.
464 *Food Chem.* **196**, 885-896 (2016).
- 465 8. Yuan, H., Zhang, J., Nageswaran, D. & Li, L. Carotenoid metabolism and
466 regulation in horticultural crops. *Hortic Res.* **2**, 15036 (2015).
- 467 9. Isaacson, T., Ohad, I., Beyer, P. & Hirschberg, J. Analysis in vitro of the enzyme
468 CRTISO establishes a poly-cis-carotenoid biosynthesis pathway in plants. *Plant*

- 469 *Physiol.* **136**, 4246-4255 (2004).
- 470 10. Lee, J. M. et al. Combined transcriptome, genetic diversity and metabolite profiling
471 in tomato fruit reveals that the ethylene response factor SlERF6 plays an important
472 role in ripening and carotenoid accumulation. *Plant J.* **70**, 191-204 (2012).
- 473 11. Llorente, B. et al. Tomato fruit carotenoid biosynthesis is adjusted to actual
474 ripening progression by a light-dependent mechanism. *Plant J.* **85**, 107-119 (2016).
- 475 12. Stanley, L. E. et al. A tetratricopeptide repeat protein regulates carotenoid
476 biosynthesis and chromoplast development in Monkeyflower (*Mimulus*). *Plant*
477 *Cell* **32**, 1536-1555 (2020).
- 478 13. Lu, S., Ye, J. & Zhu, K. A fruit ripening-associated transcription factor CsMADS5
479 positively regulates carotenoid biosynthesis in citrus. *J. Exp. Bot.* **72**, 3028-43
480 (2021).
- 481 14. Lu, S. et al. The Citrus transcription factor CsMADS6 modulates carotenoid
482 metabolism by directly regulating carotenogenic genes. *Plant Physiol.* **176**, 2657-
483 2676 (2018).
- 484 15. Zhu, F. et al. An R2R3-MYB transcription factor represses the transformation of
485 alpha- and beta-branch carotenoids by negatively regulating expression of *CrBCH2*
486 and *CrNCED5* in flavedo of citrus reticulata. *New Phytol.* **216**, 178-192 (2017).
- 487 16. Fu, C. C. et al. The Papaya Transcription Factor CpNAC1 Modulates Carotenoid
488 Biosynthesis through Activating Phytoene Desaturase Genes CpPDS2/4 during
489 Fruit Ripening. *J. Agri. & Food Chem.* **64**, 5454-63 (2016).
- 490 17. Fu, C. C., Han, Y. C., Kuang, J. F., Chen, J. Y. & Lu, W. J. Papaya CpEIN3a and

- 491 CpNAC2 co-operatively regulate carotenoid biosynthesis-related genes CpPDS2/4,
492 CpLCY-e and CpCHY-b during fruit ripening. *Plant Cell Physiol.* **58**, 2155-2165
493 (2017).
- 494 18. Zhou, D. et al. Papaya CpbHLH1/2 regulate carotenoid biosynthesis-related genes
495 during papaya fruit ripening. *Hortic Res.* **6**, 80 (2019).
- 496 19. Ampomah-Dwamena, C., Thrimawithana, A. H., Dejnopratt, S., Lewis, D., Espley,
497 R. V. & Allan, A. C. A kiwifruit (*Actinidia deliciosa*) R2R3-MYB transcription
498 factor modulates chlorophyll and carotenoid accumulation. *New Phytol.* **221**, 309-
499 325 (2019).
- 500 20. Sagawa, J. M. et al. An R2R3-MYB transcription factor regulates carotenoid
501 pigmentation in *Mimulus lewisii* flowers. *New Phytol.* **209**, 1049-1057 (2016).
- 502 21. Lado, J., Zacarias, L. and Rodrigo, M. J. Regulation of Carotenoid Biosynthesis
503 During Fruit Development. *Subcell Biochem.* **79**, 161-198 (2016).
- 504 22. Cruz, A. B. et al. Light, ethylene and auxin signaling interaction regulates
505 carotenoid biosynthesis during tomato fruit ripening. *Front Plant Sci.* **9**, 1370
506 (2018).
- 507 23. Yoo, H. J., Kim, J. H., Park, K. S., Son, J. E. & Lee, J. M. Light-controlled fruit
508 pigmentation and flavor volatiles in tomato and bell pepper. *Antioxidants* **9**, 14
509 (2019).
- 510 24. Liu, T. et al. Improved peach peel color development by fruit bagging. Enhanced
511 expression of anthocyanin biosynthetic and regulatory genes using white non-
512 woven polypropylene as replacement for yellow paper. *Sci. Hortic.* **184**, 142-148

- 513 (2015).
- 514 25. Lado, J. et al. Light regulation of carotenoid biosynthesis in the peel of mandarin
515 and sweet orange fruits. *Front Plant Sci.* **10**, 1288 (2019).
- 516 26. Hu, L., Yang, C., Zhang, L., Feng, J. & Xi, W. Effect of light-emitting diodes and
517 ultraviolet irradiation on the soluble sugar, organic acid, and carotenoid content of
518 postharvest sweet oranges (*Citrus sinensis* (L.) Osbeck). *Molecules* **24**, 3440
519 (2019).
- 520 27. Liu, L. H., Zabarar, D., Bennett, L. E., Aguas, P. & Woonton, B.W. Effects of
521 UV-C, red light and sun light on the carotenoid content and physical qualities of
522 tomatoes during post-harvest storage. *Food Chem.* **115**, 495-500 (2009).
- 523 28. Ma, G. et al. Effect of blue and red LED light irradiation on beta-cryptoxanthin
524 accumulation in the flavedo of citrus fruits. *J. Agric. Food Chem.* **60**, 197-201
525 (2012).
- 526 29. Llorente, B., Martinez-Garcia, J. F., Stange, C. & Rodriguez-Concepcion, M.,
527 Illuminating colors: regulation of carotenoid biosynthesis and accumulation by
528 light. *Curr. Opin. Plant Biol.* **37**, 49-55 (2017).
- 529 30. Cronje, P. J. R., Barry, G. H. & Huysamer, M. Canopy position affects pigment
530 expression and accumulation of flavedo carbohydrates of 'Nules Clementine'
531 mandarin fruit, thereby affecting rind condition. *J. Am. Soc. Hortic. Sci.* **138**, 217–
532 224 (2013).
- 533 31. Kondo, S. et al. Abscisic acid metabolism and anthocyanin synthesis in grape skin
534 are affected by light emitting diode (LED) irradiation at night. *J. Plant Physiol.*

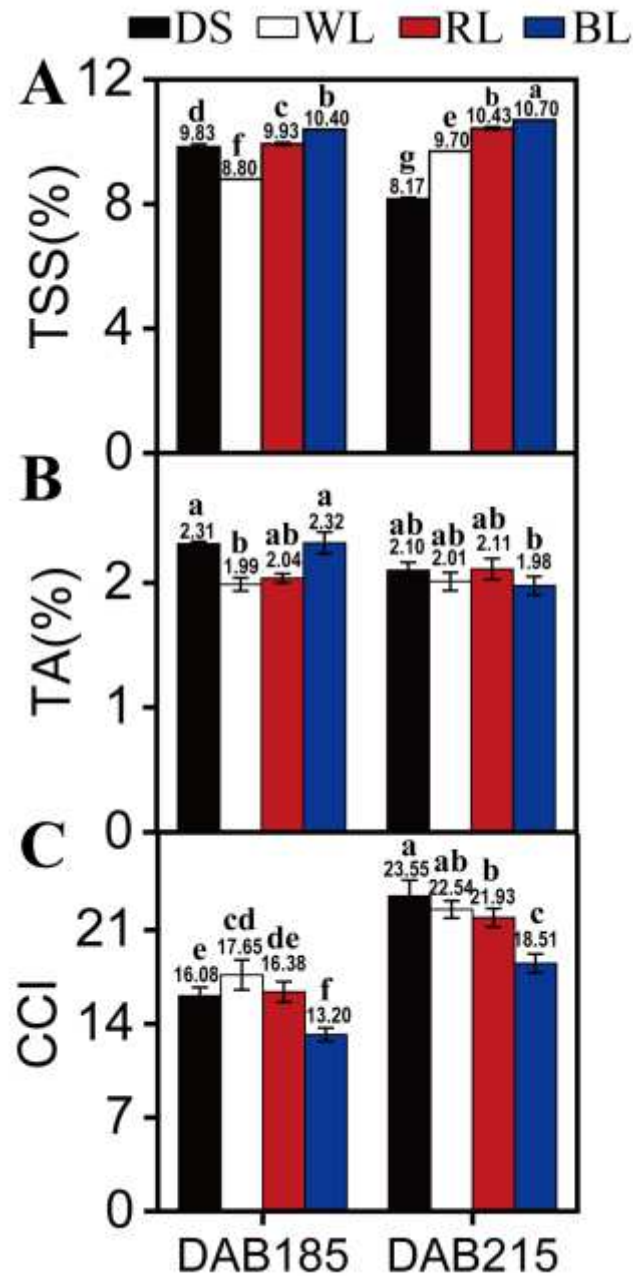
- 535 **171**, 823-829 (2014).
- 536 32. Zhang, L. et al. Regulation of carotenoid accumulation and the expression of
537 carotenoid metabolic genes in citrus juice sacs in vitro. *J. Exp. Bot.* **63**, 871-886
538 (2012).
- 539 33. Lintig, J. V. et al. Light-dependent regulation of carotenoid biosynthesis occurs at
540 the level of phytoene synthase expression and is mediated by phytochrome in
541 *Sinapis alba* and *Arabidopsis thaliana* seedlings. *Plant J.* **12**, 625–634 (1997).
- 542 34. Toledo-Ortiz, G., Huq, E. & Rodriguez-Concepcion, M. Direct regulation of
543 phytoene synthase gene expression and carotenoid biosynthesis by phytochrome-
544 interacting factors. *Proc. Natl. Acad. Sci. U. S. A.* **107**, 11626-11631 (2010).
- 545 35. Xie, B. X. et al. Supplemental blue and red light promote lycopene synthesis in
546 tomato fruits. *J. Integr. Agric.* **18**, 590-598 (2019).
- 547 36. Rosado, D., Trench, B., Bianchetti, R. E., Zuccarelli, R. & Rossi, M.
548 Downregulation of phytochrome-interacting factor 4 influences plant development
549 and fruit production. *Plant physiol.* **181**, 1360-1370 (2019).
- 550 37. Fujisawa, M., Nakano, T., Shima, Y. & Ito, Y. A large-scale identification of direct
551 targets of the tomato MADS box transcription factor RIPENING INHIBITOR
552 reveals the regulation of fruit ripening. *Plant Cell* **25**, 371-386 (2013).
- 553 38. Fujisawa, M. et al. Transcriptional Regulation of fruit ripening by tomato
554 FRUITFULL homologs and associated MADS box proteins. *Plant Cell* **26**, 89-101
555 (2014).
- 556 39. Wang, X. et al. PpERF3 positively regulates ABA biosynthesis by activating

- 557 *PpNCED2/3* transcription during fruit ripening in peach. *Hortic Res.* **6**, 19 (2019).
- 558 40. Welsch, R., Maass, D., Voegel, T., DellaPenna, D. & Beyer, P. Transcription factor
559 RAP2.2 and its interacting partner SINAT2: stable elements in the carotenogenesis
560 of Arabidopsis leaves. *Plant Physiol.* **145**, 1073–1085 (2007).
- 561 41. Mohanty, B. et al. Light-specific transcriptional regulation of the accumulation of
562 carotenoids and phenolic compounds in rice leaves. *Plant Signal Behav.* **11**, 3002-
563 3020 (2016).
- 564 42. Kou, X. et al. SNAC4 and SNAC9 transcription factors show contrasting effects
565 on tomato carotenoids biosynthesis and softening. *Postharvest Biol. Technol.* **144**,
566 9-19 (2018).
- 567 43. Zhu, M., et al. A new tomato NAC (NAM/ATAF1/2/CUC2) transcription factor,
568 SINAC4, functions as a positive regulator of fruit ripening and carotenoid
569 accumulation. *Plant Cell Physiol.* **55**, 119-135 (2014).
- 570 44. Ma, N. et al. Overexpression of tomato SINAC1 transcription factor alters fruit
571 pigmentation and softening. *BMC Plant Biol.* **14**, 351 (2014).
- 572 45. Wang, Z., Rashotte, A. M. & Dane, F. *Citrullus colocynthis* NAC transcription
573 factors CcNAC1 and CcNAC2 are involved in light and auxin signaling. *Plant Cell*
574 *Rep.* **33**, 1673-1686 (2014).
- 575 46. Gong, J. et al. Red light-induced kumquat fruit colouration is attributable to
576 increased carotenoid metabolism regulated by FcrNAC22. *J. Exp. Bot.* erab283
577 (2021).
- 578 47. Han, Y. et al. Characterization of OfWRKY3, a transcription factor that positively

- 579 regulates the carotenoid cleavage dioxygenase gene *OfCCD4* in *Osmanthus*
580 *fragrans*. *Plant Mol. Biol.* **91**, 485-496 (2016).
- 581 48. Zheng, H., Zhang, Q., Quan, J., Zheng, Q. & Xi, W. Determination of sugars,
582 organic acids, aroma components, and carotenoids in grapefruit pulps. *Food Chem.*
583 **205**, 112-121 (2016).
- 584 49. Kim, D., Langmead, B. & Salzberg, S. L. HISAT: a fast spliced aligner with low
585 memory requirements. *Nat. Methods* **12**, 357-360 (2015).
- 586 50. Li, B. & Dewey, C. N. RSEM: accurate transcript quantification from RNA-Seq
587 data with or without a reference genome. *BMC Bioinformatics* **12**, 323 (2011).
- 588 51. Zhang, Q. et al. Transcriptional regulatory networks controlling taste and aroma
589 quality of apricot (*Prunus armeniaca* L.) fruit during ripening. *BMC Genom.* **20**,
590 45 (2019).
- 591 52. Langfelder, P. & Horvath, S. WGCNA: an R package for weighted correlation
592 network analysis. *BMC Bioinformatics* **9**, 559 (2008).

593

594 **Figures and figure legends**



595

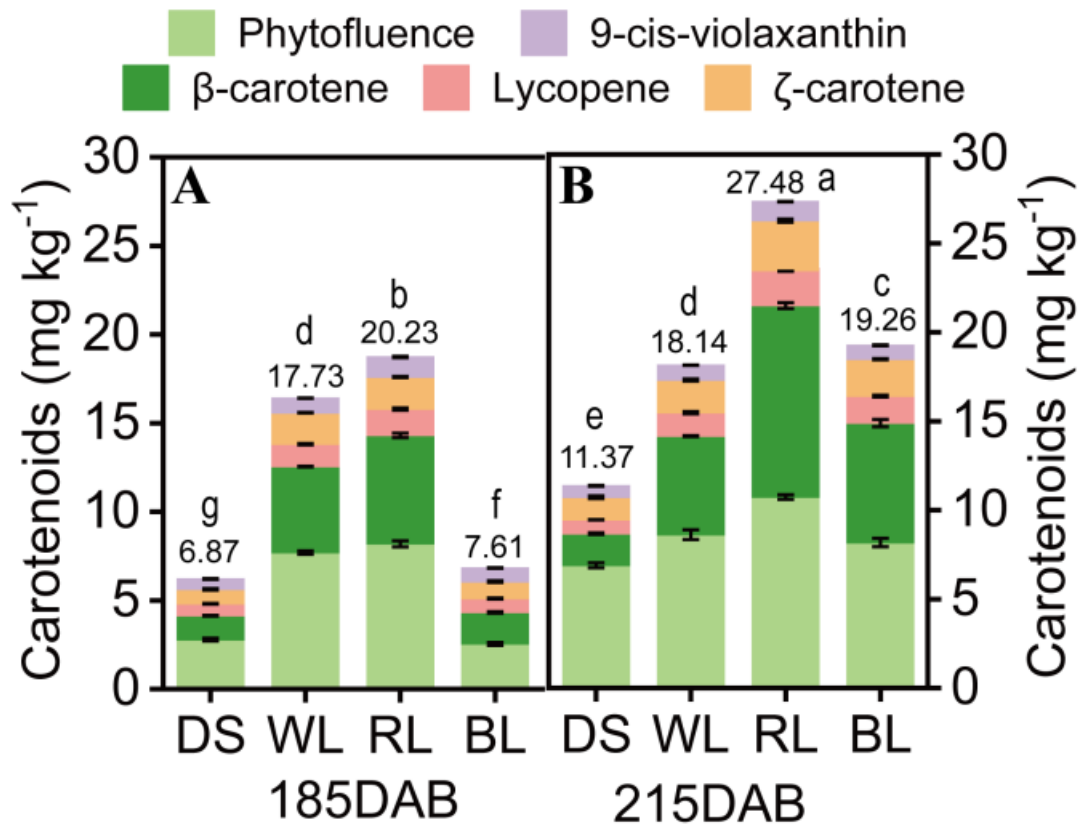
596 **Fig. 1** Effect of grapefruit bagged with four light-transmitting bags on the TSS content

597 (A), TA content (B) and CCI (C) of grapefruits during ripening. Error bar indicate

598 standard error from three biological replicates (n = 3). DS: dark-shade treatment; RL:

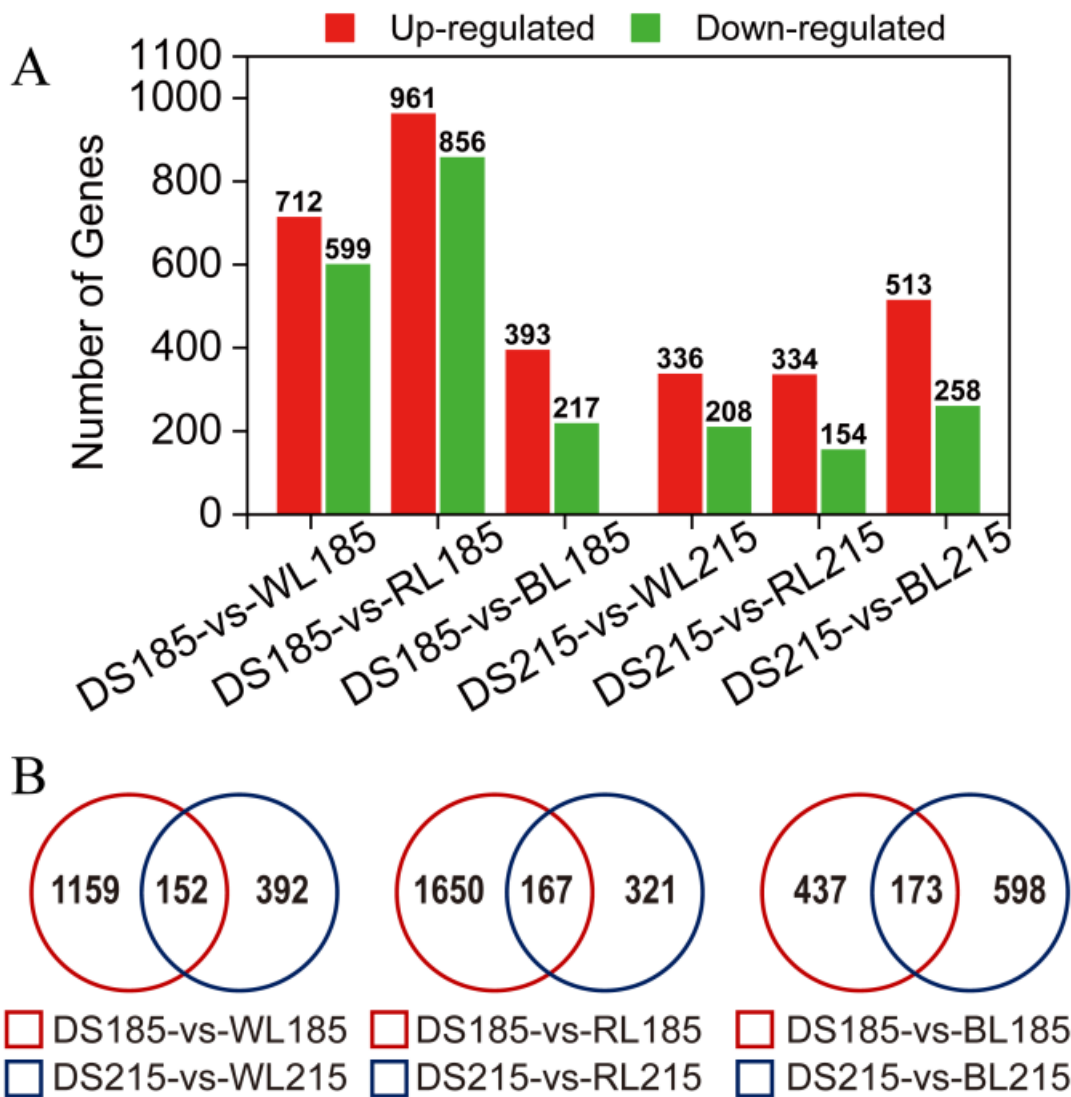
599 red-light treatment; BL: blue-light treatment; WL: white-light treatment. Different

600 letters indicate statistically significant difference in one-way ANOVA analysis.



601

602 **Fig. 2** Effects of different light treatments on content of carotenoid, including β-
 603 carotene, phytofluene, ζ-carotene, lycopene, and 9-*cis*-violaxanthin content during
 604 grapefruit ripening. Error bars indicate the standard error from three biological
 605 replicates ($n = 3$). DS: dark-shade treatment; RL: red-light treatment; BL: blue-light
 606 treatment; WL: white-light treatment. Different letters indicate statistically significant
 607 difference in one-way ANOVA analysis.



608

609 **Fig. 3** Profiling the changed genes and DEGs between grapefruit at different ripening

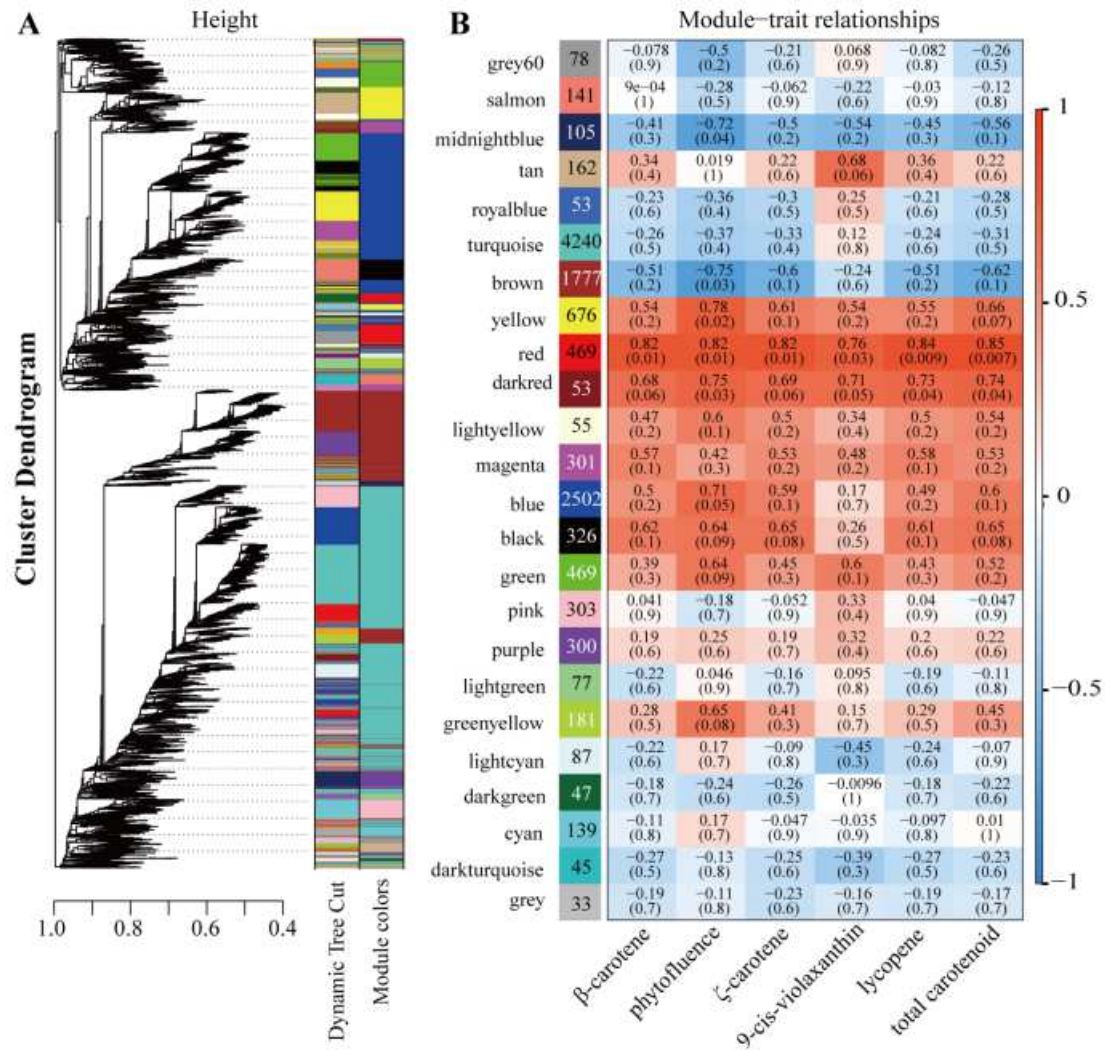
610 stages. (A) The histogram presents the number of upregulated and downregulated genes

611 between samples during grapefruit ripening. (B) Venn diagram for DEGs between

612 grapefruit samples at two ripening stages. “A” is the control group and “B” was the

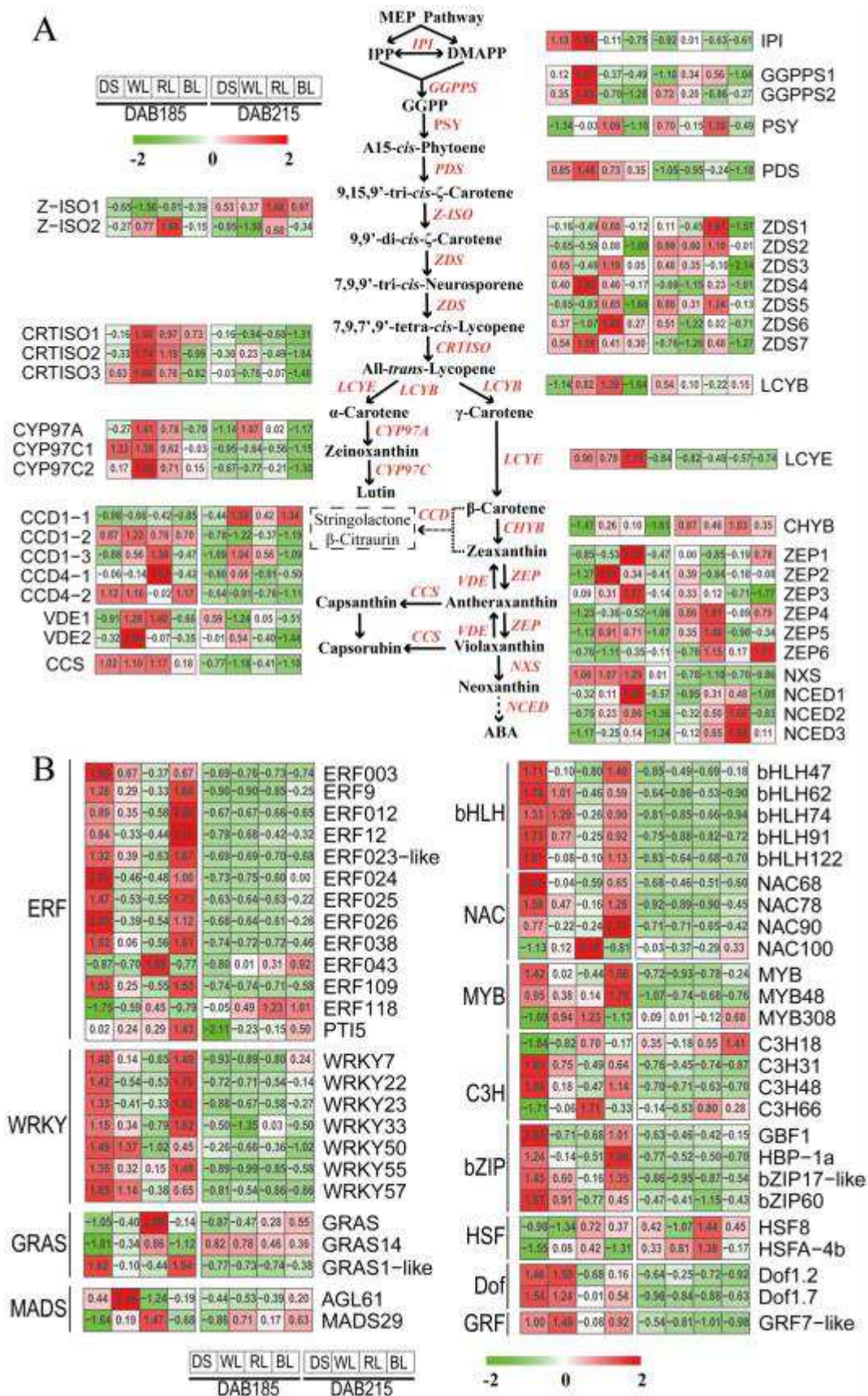
613 treatment group in “A-vs-B”. DS: dark-shade treatment; RL: red-light treatment; BL:

614 blue-light treatment; WL: white-light treatment.



615

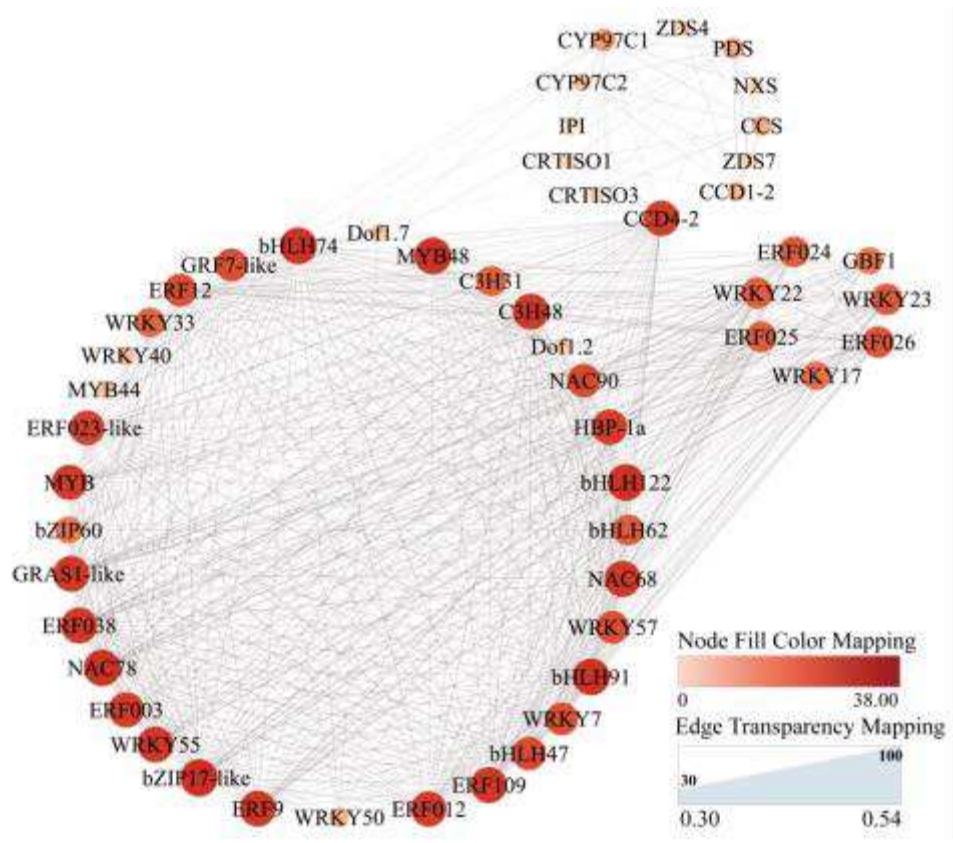
616 **Fig. 4** Weighted gene co-expression network analysis of grapefruit during ripening
 617 under different light-transmittance treatments. A. Hierarchical clustering tree displays
 618 twenty-four modules of co-expressed genes, in which each leaf represents one gene. B.
 619 Modules related to carotenoid and corresponding p -values. The left panel indicates
 620 twenty-four modules and the number of genes contained by each module. The right
 621 panel displays a color scale for module or trait correlations from -1 to 1 .



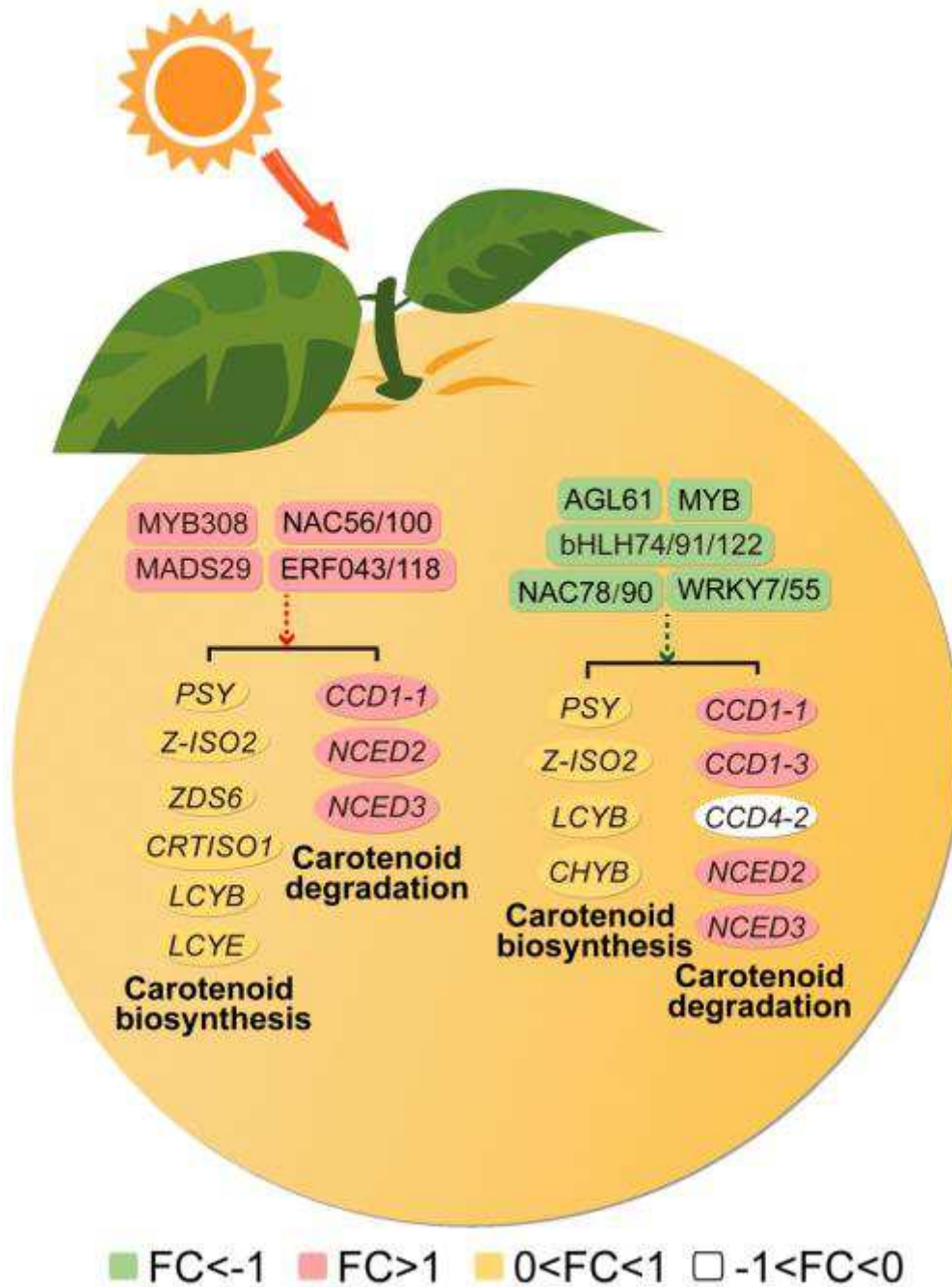
622

623 **Fig. 5** Heatmap analysis of structural genes (A) and transcriptional factors (B) correlated

624 with carotenoid metabolism during grapefruit ripening. Rows and columns indicate
 625 gene names and samples in the heatmap, respectively. Red, white and green represent
 626 high, medium and low expression level for genes. DS: dark-shade treatment; RL: red-
 627 light treatment; BL: blue-light treatment; WL: white-light treatment.



629 **Fig. 6** The co-expression network of TFs and structural genes related to carotenoid
 630 metabolism. Dot sizes and colors represent the numbers for correlated genes.



631

632 **Fig. 7** The proposed models of carotenoid metabolism mediated by red light during

633 grapefruit ripening. Pale pink and light green rounded rectangle, respectively,

634 represents up- and down-regulated TFs in response to RL. Red and green arrow indicate

635 positive and negative regulation of TFs on structural genes, respectively. Oval suggests

636 structural genes in carotenoid metabolic pathway. Different colors represent up- and
637 down-regulation level for genes in response to RL.
638

Supplementary Files

This is a list of supplementary files associated with this preprint. Click to download.

- [Supplemetaryfigures.pdf](#)
- [Supplemetarytables.docx](#)